JACS
JOURNAL OF THE AMERICAN CHEMICAL SOCIETY

Communication

pubs.acs.org/JACS

Temperature-Directed Self-Assembly of Multifunctional Polymeric Tadpoles

Valentin A. Bobrin and Michael J. Monteiro*

Australian Institute for Bioengineering and Nanotechnology, The University of Queensland, St. Lucia, Brisbane, Queensland 4072, Australia

Supporting Information

ABSTRACT: Multicompartment tadpole nano-objects are a rare and intriguing class of structures with potential in a wide range of applications. Here, we demonstrate the synthesis of chemically multifunctional polymer tadpoles made at high weight fractions of polymer (>10 wt %). The tadpoles are synthesized using two different thermoresponsive MacroCTAs with either alkyne or pyridyldisulfide end-groups, allowing chemical functionality in the head, tail, or both. Water-soluble molecules or polymers were coupled to either the head, tail or both without a change in tadpole configuration. In addition, the tadpoles can be dried, rehydrated, and stored in water for 5 months without a change in shape. This method represents a new and an important synthetic development in the design of nano-objects.

Building nanostructures with controlled geometry and multiple compartments with a variety of chemical functionalities represent an important development in the design of nano-objects.[1−5] These types of new structures will further extend the use of nano-objects in biological,[6] photonics,[7] and chemical[8] applications. The tadpole structure has a unique geometric shape with two main compartments: the head and the tail. In biology, tadpoles comprise a class of highly specialized entities, including sperm cells, bacteria, and bacteriophages. The head contains genetic material, and the tail allows attachment to cells (e.g., bacteriophage) or enhances mobility by allowing the tadpole to swim (e.g., sperm). Nanoscale designed tadpoles with orthogonal functionality in the head and tail will have potential as *in vivo* drug delivery systems. The long and flexible worm-like tail structure could significantly increase the blood circulation time as compared to spherical or stealth vesicles,[9,10] while the head could be loaded with small molecule or peptide drugs.

The most common method to make polymeric tadpoles is via controlled folding of single polymer chains.[11−13] The size of these structures is small (<10 nm), and due to such small dimensions will not capture the advantageous properties of tadpoles described above. There are only a few rare examples of the aqueous synthesis of polymeric tadpole structures on the nanoscale with flexible and long tails.[1,3,14−16] An early example utilized miktoarm star polymers to produce a tadpole with a vesicle as the head and a long segmented worm micelle.[14,15] More recently, kinetic control of the self-assembly of block copolymers allowed the construction of tadpole structures.[1,3,16] However, the tadpole polymers in these examples were formed under high dilution (<0.02 wt %), and in many cases other dominant structures (e.g., spheres or vesicles) were observed alongside the tadpoles by transmission electron microscopy (TEM). Currently, there is no method for the rapid production of tadpoles in water at a high weight fraction of polymer and with chemical functionality in both head and tail.

Herein, we report a method to produce chemically multifunctional tadpoles directly in water at a high weight fraction of polymer using a one-step reversible addition−fragmentation chain transfer (RAFT)-mediated dispersion polymerization (Scheme 1). Previously, this method, denoted as the temperature-directed morphology transformation (TDMT),[17−19] enabled the production of a wide variety of nano-objects, including worms with multiple types of chemical functionality on the surface.[20] In the tadpole synthesis, we used multiple thermoresponsive polyisopropylacrylamide (PNIPAM) macro-RAFT agents (MacroCTAs) with a low and a high lower critical solution temperature (LCST), with all LCSTs below the polymerization temperature (see Figure S13). The LCST was controlled through either end-group or copolymer composition: incorporation of hydrophobic units (e.g., styrene, STY) results in lowering the LCST, whereas hydrophilic units (e.g., dimethyl acrylamide, DMA) increase the LCST.[21−24] By dissolving the MacroCTAs in water and heating to a temperature above the LCSTs, the MacroCTAs formed seed particles that were the polymerization loci[25,26] for the chain extension with styrene monomer. After polymerization, latex spherical particles formed, comprising of diblock copolymers in which one block was the MacroCTAs and the other polystyrene (PSTY). The MacroCTA and PSTY block lengths were chosen to form a cylindrical tail;[18,20,27] a detailed phase diagram was described using the TDMT method with varying PNIPAM and PSTY block lengths.[18] To produce the tadpole structure, in the presence of a small amount of plastizer (i.e., toluene) for PSTY, we cooled the latex from the polymerization temperature of 70 to 34 °C, which was below that of the high LCST MacroCTAs but above that of the low LCST MacroCTAs. The tadpoles were produced at ∼10 wt % and with chemical functionality in both head and tail. The head consisted of collapsed PNIPAM globules from the low LCST MacroCTA blocks and the tail of the highly water-soluble PNIPAM chains from the high LCST MacroCTA blocks. Since the LCST of tail PNIPAM blocks were >34 °C, the R-groups on the PNIPAM chain-ends resided on the tail surface,[20] whereas the R-groups from the low LCST PNIPAM should be located

Received: October 21, 2015
Published: December 5, 2015

DOI: 10.1021/jacs.5b11037
J. Am. Chem. Soc. 2015, 137, 15652−15655

Scheme 1. Synthesis of Multifunctional Nano-Tadpoles through One-Pot RAFT-Mediated Emulsion Polymerization with Cooling to 34 °C[a]

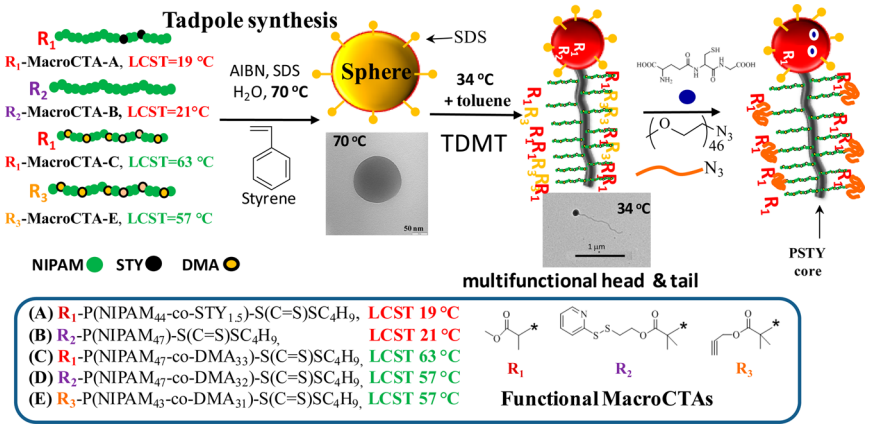

[a]The average number of styrene units in MacroCTA-A was determined from 1H NMR and supported from MALDI-ToF data in Figure S11.

Table 1. Synthesis of Tadpoles by RAFT-Mediated Emulsion Polymerization at 70 °C in Water for 4 h Using SDS as Surfactant and AIBN as Initiator and Then Cooling to 34 °C

					SEC triple detection (DMAc)[d]			
expt	MacroCTA[a]	weight ratio[b]	conv (%)[c]	STY units ^{1}H NMR	M_n	PDI	$D_{h,DLS}$[e]	PDI_{DLS}[e]
1	A:C	0.5:0.5	68	39	9780	1.11	117	0.079
2	A:C	0.4:0.6	73	44	10800	1.11	114	0.101
3	A:C:D	0.5:0.25:0.25	72	45	10950	1.14	112	0.096
4	A:C:E	0.5:0.25:0.25	84	50	11280	1.10	114	0.099
5	A:E	0.5:0.5	73	45	11095	1.10	131	0.079
6	A:C:D:E	0.5:0.167:0.167:0.167	72	44	11900	1.10	117	0.094
7	A:C:D:E	0.5:0.25:0.125:0.125	73	45	11700	1.10	119	0.081
8	A:D:E	0.5:0.25:0.25	81	48	11980	1.10	112	0.097
9	A:B:C	0.4:0.1:0.5	64	35	11600	1.09	136	0.084
10	A:B:C:E	0.4:0.1:0.25:0.25	82	45	13840	1.09	123	0.099

[a]MacroCTAs: A = R_1-P(NIPAM$_{44}$-*co*-STY$_{1.5}$)-S(C═S)C$_4$H$_9$, B = R_2-PNIPAM$_{47}$-S(C═S)C$_4$H$_9$, C = R_1-P(NIPAM$_{47}$-*co*-DMA$_{33}$)-S(C═S)C$_4$H$_9$, D = R_2-P(NIPAM$_{47}$-*co*-DMA$_{32}$)-S(C═S)C$_4$H$_9$, E = R_3-P(NIPAM$_{43}$-*co*-DMA$_{31}$)-S(C═S)C$_4$H$_9$. [b]Weight ratio of MacroCTAs. [c]Conversions obtained by gravimetry. [d]Eluent = DMAc + 0.03 wt % LiCl; polystyrene calibration curve. [e]Particle size ($D_{h,DLS}$) and dispersity index (PDI_{DLS}) of latex measured by DLS at 70 °C immediately after the reaction. $PDI_{(DLS)}$ < 0.1 means narrow distribution.

within the head. We further demonstrated that reactions with the R-groups resulted in coupling of polymer chains or small molecules to both the head and the tail.

In the first example (expt 1 in Table 1), we used two ester chain-end functional MacroCTAs: one with a high LCST (63 °C) just below the polymerization temperature (i.e., R_1-MacroCTA-C), and the other with a low LCST of 19 °C (i.e., R_1-MacroCTA-A). See Figure S13 for determination of the LCSTs. After the polymerization of styrene at 70 °C, two diblocks: (i) P((NIPAM$_{44}$-*co*-STY$_{1.5}$)-*b*-STY$_{39}$) and (ii) P-((NIPAM$_{47}$-*co*-DMA$_{33}$)-*b*-STY$_{39}$) formed simultaneously producing a cumulative molecular weight distribution with a number-average molecular weight (M_n) of 9780 (close to M_n theory) and polydispersity index (PDI) of 1.11. The resulting spherical particles (Figure 1A) had a hydrodynamic diameter ($D_{h,DLS}$) of 117 nm with a PDI_{DLS} of 0.079 as measured by dynamic light scattering (DLS). (Note: a PDI_{DLS} <0.1 represents a narrow particle size distribution). The narrow particle size distribution was due to the superswelling effect by incorporation of styrene units in R_1-MacroCTA-A.[28,29] The size measured by DLS closely correlated to the $D_{h,TEM}$ determined from TEM (Figure 1A). The reaction vessel containing the latex was opened to the atmosphere and kept at 70 °C for 4 h to remove all nonpolymerized styrene.[17] Upon cooling to 34 °C in the presence of a small amount of toluene, to plasticize the PSTY chains, these spherical particles transformed into tadpoles (Figure 1B). The optimized toluene amounts to allow formation of the tadpoles was >20 μL/mL (see Figure S27). At lower amounts of toluene, the structures were kinetically trapped owing to the glassy PSTY chains, whereas above the glass state of PSTY (i.e., at a high toluene amount) the structures transitioned toward their thermodynamic equilibrium morphology. The average head size decreased from 116 nm ($D_{h,TEM}$) to 100 nm (Figure 1C), which was expected due to the translocation of the high LCST diblocks to the tail. The tadpoles could be freeze-dried to remove any toluene and rehydrated without change in structure (see Figure S17). In addition, the tadpoles showed no structural change after rehydration and storage in water for 5 months at ambient temperature (Figure 1D), suggesting that these structures were stabilized by the high glass transition temperature of the PSTY in the core.[17,20]

To determine whether the tail extrudes from the head upon cooling from 70 to 34 °C or whether it rearranges to a tadpole when held at 34 °C for an extended period, the latex from expt 1 (in Table 1) was cooled to four temperatures. The four temperatures (57, 52, 45, and 34 °C) were selected to study

DOI: 10.1021/jacs.5b11037
J. Am. Chem. Soc. 2015, 137, 15652−15655

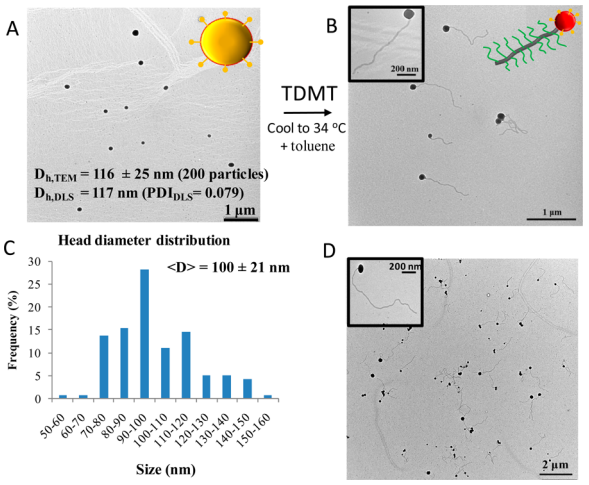

Figure 1. TEM images from expt 1 (Table 1) after removal of unpolymerized styrene at 70 °C. (A) Latex placed on the grid at 70 °C. (B) Latex cooled and placed on the grid to 34 °C. (C) Head diameter measured from TEM in graph B. (D) Latex cooled to 34 °C, freeze-dried, rehydrated, and then stored in water at room temperature for 5 months.

the transition of R_1-MacroCTA-C from a collapsed globule to a water-soluble coil conformation along curve b in Figure 2. The latex was cooled from 70 °C to the selected temperature and annealed at that temperature for 15 h before being placed on a TEM grid. The TEMs in Figure 2 showed that the spherical particles at 70 °C slowly transformed into tadpoles. A decrease in the annealing temperature from 57 to 45 °C resulted in an increase in the tail length. It should be noted that in this temperature range, in which the PNIPAM was still in transition from globule to coil, there were still many spheres observed (see Figure S18). Only at 34 °C, which was well below the LCST of R_1-MacroCTA-C, do we observe near full transformation to tadpoles with long and flexible tails. This clearly showed that temperature was the driver for tadpole formation. Expt 2 (Table 1) showed that the ratio of R_1-MacroCTA-A to R_1-MacroCTA-C

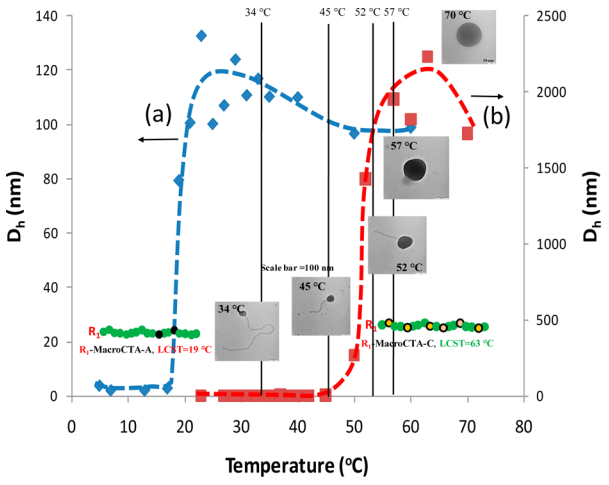

Figure 2. Hydrodynamic diameter of R_1-MacroCTA-A (curve a) and R_1-MacroCTA-C (curve b) with temperature as measured by DLS. TEM images represent latex from expt 1 (Table 1), cooled from 70 to 34 °C (i.e., consecutive cooling from 70, 57, 52, 45, and 34 °C corresponding to LCST change of R_1-MacroCTA-C); extrusion of tail from the head.

could be changed, enabling the stoichiometry variation of the R-groups in the head versus the tail.

The next set of experiments involved the use of multiple MacroCTAs with different R-groups (see Scheme 1 and Table 1). After polymerization with styrene and subsequent cooling to 34 °C, tadpole structures formed (see Figure S16) in which the R-groups could be located either in the head, tail or both. All experiments showed 'living' radical polymerization behavior with the M_n close to theory and narrow molecular weight distributions (i.e., PDIs < 1.3) and the hydrodynamic diameter ranged from 112 to 136 nm with narrow size distributions (see Table 1). This demonstrated that the number and types of MacroCTAs do not influence the RAFT polymerization and particle formation. The tadpole from expt 3 contained the R-groups from MacroCTAs A, C, and D, in which the tail consisted of a pyridyl disulfide (PDS) in 25 wt % that could be further used in thio-disulfide exchange or thiol-ene reactions. The ratio of R_2-MacroCTA-D could be increased to 50 wt % on the tail of the tadpole (data not shown). Alkyne groups, for copper-catalyzed alkyne-azide cycloaddition (CuAAC) 'click' reactions, were directed to the surface of the tail by using R_3-MacroCTA-E with an LCST much higher than 34 °C (expts 4 and 5 in Table 1). We could further direct the placement and ratio of both alkyne and PDS groups simultaneously on the tail of the tadpole (expts 6–8), producing a multifunctional tail with orthogonal coupling functional groups. Incorporation of the PDS R-group within the head (expt 9) and an ester R-group on the tail also led to the formation of stable tadpoles. Expt 10 demonstrated the versatility of our method, in which we could incorporate a PDS functionality within the head and alkyne functionality on the tail. The ratio, number, and types of R-groups can be readily programmed through simply varying the ratio, number, and types of functional MacroCTAs.

To demonstrate the chemical reactivity of the PDS and alkyne groups in the head and tail, we coupled the tadpole structures (from expts 3, 5, and 9) to various water-soluble thiol and azide functional molecules (Figure 3). Figure 3A showed that coupling L-GSH, 1-thioglycerol, and polydimethyl acrylamide ($PDMA_{115}$-SH) to the tail of the tadpole (expt 3) gave coupling efficiencies of ~60%. The reaction of a thiol reagent with PDS groups produced a disulfide and 2-mercaptopyridine. The large extinction coefficient of 2-mercaptopyridine (ε = 7360 $M^{-1}\cdot cm^{-1}$ at λ = 342 nm) was used to quantitatively determine the coupling efficiency (see Figure S19). The coupling efficiency of 60% corresponds to low reaction efficiency for this type of reaction.[20] The reaction between the alkyne-functional tail (expt 5) and a PEG-N_3 gave near quantitative coupling from the loss of the PEG-N_3 and formation of a higher molecular weight polymer as observed in the size exclusion chromatograms[30] (Figure 3B). It was further found that no change in the tadpole after coupling was observed (Figures S22, S23, and S26). The next reaction between the thiol-functional molecules and the PDS groups within the head of the tadpole (expt 9) gave coupling efficiencies of 40–50% (Figure 3C). This was not an unexpected result since PNIPAM in its globular state still contains a considerable amount of bound water (~60%),[31−33] allowing diffusion of water-soluble compounds into the head to react with the PDS groups. Importantly, the tadpole structure and especially the size of the head did not change after the coupling reactions with the three water-soluble reagents (Figure S24).

In conclusion, we have demonstrated a technique to directly prepare tadpole structures in water at a weight fraction of ~10 wt % with a multifunctional head and tail. The molecular weight and molecular weight distribution were well-controlled (i.e.,

DOI: 10.1021/jacs.5b11037
J. Am. Chem. Soc. 2015, 137, 15652−15655

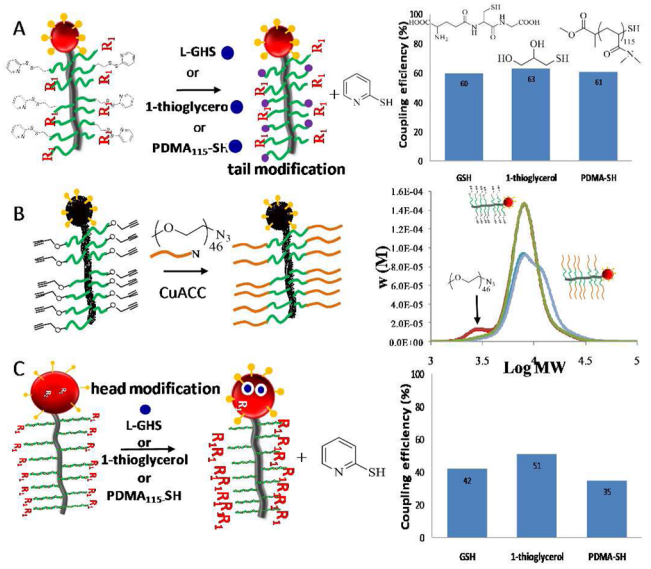

Figure 3. Schematic showing the modification of functional tadpoles with either L-GHS, 1-thioglycerol, $PDMA_{115}$-SH, or PEG-N_3. (A) Reaction with PDS tail from expt 3 (Table 1); (B) reaction with alkyne tail from expt 5, SEC traces: green curve is starting latex polymer only, red curve is PEG-N_3 + latex polymer at t = 0 h, blue curve is coupling reaction between PEG-N_3 and alkyne on latex polymer; and (C) reaction with PDS head from expt 9.

proceeded via 'living' radical polymerization), and the particle sizes were close to ∼110 nm with narrow particle size distributions. We could control not only the types of R-groups but also their stoichiometry on the tail and within the head of the tadpole. Further coupling of these R-groups to water-soluble molecules showed high coupling efficiencies to the R-groups on the tail and moderate coupling in the head. The tadpole structures remained unchanged after these coupling reactions, suggesting that their multifunctionality and structural robustness could have utility in drug and vaccine delivery, nanoreactors, tissue engineering, diagnostics, rheology modifiers, and many other applications.

■ ASSOCIATED CONTENT

Supporting Information

The Supporting Information is available free of charge on the ACS Publications website at DOI: 10.1021/jacs.5b11037.

Materials, synthetic procedures, characterization of compounds and polymers (PDF)

■ AUTHOR INFORMATION

Corresponding Author

*m.monteiro@uq.edu.au

Notes

The authors declare no competing financial interest.

■ ACKNOWLEDGMENTS

Australian Research Council (ARC) DP150101874.

■ REFERENCES

(1) Pochan, D. J.; Zhu, J. H.; Zhang, K.; Wooley, K. L.; Miesch, C.; Emrick, T. *Soft Matter* **2011**, *7*, 2500.
(2) Moughton, A. O.; Hillmyer, M. A.; Lodge, T. P. *Macromolecules* **2012**, *45*, 2.
(3) Zhu, J. H.; Zhang, S. Y.; Zhang, K.; Wang, X. J.; Mays, J. W.; Wooley, K. L.; Pochan, D. J. *Nat. Commun.* **2013**, *4*, 2297.
(4) Qiu, H. B.; Hudson, Z. M.; Winnik, M. A.; Manners, I. *Science* **2015**, *347*, 1329.
(5) Groschel, A. H.; Muller, A. H. E. *Nanoscale* **2015**, *7*, 11841.
(6) Mitragotri, S.; Lahann, J. *Nat. Mater.* **2009**, *8*, 15.
(7) Huynh, W. U.; Dittmer, J. J.; Alivisatos, A. P. *Science* **2002**, *295*, 2425.
(8) Nishihata, Y.; Mizuki, J.; Akao, T.; Tanaka, H.; Uenishi, M.; Kimura, M.; Okamoto, T.; Hamada, N. *Nature* **2002**, *418*, 164.
(9) Geng, Y.; Dalhaimer, P.; Cai, S.; Tsai, R.; Tewari, M.; Minko, T.; Discher, D. E. *Nat. Nanotechnol.* **2007**, *2*, 249.
(10) Cai, S. S.; Vijayan, K.; Cheng, D.; Lima, E. M.; Discher, D. E. *Pharm. Res.* **2007**, *24*, 2099.
(11) Mecerreyes, D.; Lee, V.; Hawker, C. J.; Hedrick, J. L.; Wursch, A.; Volksen, W.; Magbitang, T.; Huang, E.; Miller, R. D. *Adv. Mater.* **2001**, *13*, 204.
(12) Harth, E.; Van Horn, B.; Lee, V. Y.; Germack, D. S.; Gonzales, C. P.; Miller, R. D.; Hawker, C. J. *J. Am. Chem. Soc.* **2002**, *124*, 8653.
(13) Ouchi, M.; Badi, N.; Lutz, J. F.; Sawamoto, M. *Nat. Chem.* **2011**, *3*, 917.
(14) Li, Z. B.; Hillmyer, M. A.; Lodge, T. P. *Nano Lett.* **2006**, *6*, 1245.
(15) Saito, N.; Liu, C.; Lodge, T. P.; Hillmyer, M. A. *ACS Nano* **2010**, *4*, 1907.
(16) Chen, Y.; Zhang, K.; Wang, X.; Zhang, F.; Zhu, J. H.; Mays, J. W.; Wooley, K. L.; Pochan, D. J. *Macromolecules* **2015**, *48*, 5621.
(17) Kessel, S.; Urbani, C. N.; Monteiro, M. J. *Angew. Chem., Int. Ed.* **2011**, *50*, 8082.
(18) Kessel, S.; Truong, N. P.; Jia, Z. F.; Monteiro, M. J. *J. Polym. Sci., Part A: Polym. Chem.* **2012**, *50*, 4879.
(19) Jia, Z. F.; Truong, N. P.; Monteiro, M. J. *Polym. Chem.* **2013**, *4*, 233.
(20) Jia, Z. F.; Bobrin, V. A.; Truong, N. P.; Gillard, M.; Monteiro, M. J. *J. Am. Chem. Soc.* **2014**, *136*, 5824.
(21) Neradovic, D.; Hinrichs, W. L. J.; Kettenes-van den Bosch, J. J.; Hennink, W. E. *Macromol. Rapid Commun.* **1999**, *20*, 577.
(22) Shi, Y.; van den Dungen, E. T. A.; Klumperman, B.; van Nostrum, C. F.; Hennink, W. E. *ACS Macro Lett.* **2013**, *2*, 403.
(23) Tran, N. T. D.; Truong, N. P.; Gu, W.; Jia, Z.; Cooper, M. A.; Monteiro, M. J. *Biomacromolecules* **2013**, *14*, 495.
(24) Tran, N. T. D.; Jia, Z. F.; Truong, N. P.; Cooper, M. A.; Monteiro, M. J. *Biomacromolecules* **2013**, *14*, 3463.
(25) Monteiro, M. J. *Macromolecules* **2010**, *43*, 1159.
(26) Sebakhy, K. O.; Kessel, S.; Monteiro, M. J. *Macromolecules* **2010**, *43*, 9598.
(27) Jia, Z.; Truong, N. P.; Monteiro, M. J. *Polym. Chem.* **2013**, *4*, 233.
(28) Luo, Y. W.; Tsavalas, J.; Schork, F. J. *Macromolecules* **2001**, *34*, 5501.
(29) Urbani, C. N.; Monteiro, M. J. *Macromolecules* **2009**, *42*, 3884.
(30) Monteiro, M. J. *Eur. Polym. J.* **2015**, *65*, 197.
(31) Chu, B.; Wu, C. *Macromol. Symp.* **1996**, *106*, 421.
(32) Heskins, M.; Guillet, J. E. *J. Macromol. Sci., Chem.* **1968**, *2*, 1441.
(33) Pelton, R. *J. Colloid Interface Sci.* **2010**, *348*, 673.

DOI: 10.1021/jacs.5b11037
J. Am. Chem. Soc. 2015, 137, 15652−15655